Original Article

Bisindolylmaleimide alkaloid BMA-155Cl induces autophagy and apoptosis in human hepatocarcinoma HepG-2 cells through the NF-κB p65 pathway

Xiao SUN[1, 3, #], Lin LI[1, 3, #], Hong-guang MA[2], Pu SUN[1], Qi-lin WANG[1], Ting-ting ZHANG[1], Yue-mao SHEN[3], Wei-ming ZHU[2, *], Xia LI[1, 3, *]

[1]School of Ocean, Shandong University, Weihai 264209, China; [2]School of Medicine and Pharmacy, Ocean University of China, Qingdao 266000, China; [3]School of Pharmaceutical Sciences, Shandong University, Ji-nan 250012, China

Abstract

Bisindolylmaleimides, a series of derivatives of a PKC inhibitor staurosporine, exhibit potential as anti-cancer drugs and have received considerable attention in clinical trials. This study aims to investigate the effects of a bisindolylmaleimide alkaloid 155Cl (BMA-155Cl) with a novel structure on autophagy and apoptosis in human hepatocarcinoma HepG-2 cells in vitro and in vivo. The cell poliferation was assessed with a MTT assay. Autophagy was evaluated by MDC staining and TEM analysis. Apoptosis was investigated using Annexin V-FITC/PI and DAPI staining. The antitumor effects were further evaluated in nude mice bearing HepG-2 xenografts, which received BMA-155Cl (10, 20 mg/kg, ip) for 18 days. Autophagy- and apoptosis-associated proteins and their mRNA levels were examined with Western blotting, immunohistochemistry, and RT-PCR. BMA-155Cl (2.5–20 μmol/L) inhibited the growth of HepG-2 cells with IC_{50} values of 16.62±1.34, 12.21±0.83, and 8.44±1.82 μmol/L at 24, 48, and 72 h, respectively. Furthermore, BMA-155Cl (5–20 μmol/L) dose-dependently induced autophagy and apoptosis in HepG-2 cells. The formation of autophagic vacuoles was induced by BMA-155Cl (10 μmol/L) at approximately 6 h and peaked at approximately 15 h. Pretreatment with 3-MA potentiated BMA-155Cl-mediated apoptotic cell death. This compound dose-dependently increased the mRNA and protein levels of Beclin-1, NF-κB p65, p53, and Bax, but decreased the expression of IκB and Bcl-2. Pretreatment with BAY 11-7082, a specific inhibitor of NF-κB p65, blocked BMA-155Cl-induced expression of autophagy- and apoptosis-associated proteins. BMA-155Cl administration effectively suppressed the growth of HepG-2 xenografts in vivo, and increased the protein expression levels of LC3B, Beclin-1, NF-κB p65, and Bax in vivo. We conclude that the NF-κB p65 pathway is involved in BMA-155Cl-triggered autophagy, followed by apoptosis in HepG-2 cells in vitro and in vivo. Hence, BMA-155Cl could be a promising pro-apoptotic candidate for developing as a novel anti-cancer drug.

Keywords: bisindolylmaleimides; BMA-155Cl; antitumor agents; autophagy; apoptosis; NF-κB p65; HepG-2 cells

Introduction

Apoptosis and autophagy are two different types of programmed cell death[1–3]. Apoptosis is regulated by various molecules (such as Bcl-2 family proteins), in particular by anti-apoptotic proteins (such as Bcl-2) and pro-apoptotic proteins (such as Bax and BAK). Deficiency in Bax and BAK or reduced expression of Bcl-2 suppresses apoptosis, thereby promoting tumorigenesis[2, 4]. Autophagy is an evolutionarily conserved process in response to nutrient starvation, metabolic stress, intracellular damage, exposure to chemotherapeutic agents, DNA damage, and viral infection; autophagy is important in maintaining the cellular microenvironment[5, 6]. Autophagy is also essential for long-term survival during growth factor withdrawal or cellular stress. This process serves as an adaptive response by providing nutrients and removing damaged macromolecules and organelles. However, autophagic cells coping with excessive stress may commit suicide by undergoing autophagic cell death[4].

Autophagy plays an important role in the regulation of cell survival and cell death, especially in apoptosis-signaling pathways[7]. Considerable cross-talk exists between autophagy and apoptosis. Accumulated evidence suggests that both processes share common components and promote cross-functional mutual regulation via PI3K/AKT signaling, NF-κB sig-

naling, and Bcl-2 family members[2, 8]. The cross-talk between apoptosis and autophagy is critical to cell fate but is complicated by the contradictory roles of apoptosis and autophagy under some conditions. Autophagy and apoptosis synergistically affect each other[7].

Hepatocellular carcinoma (HCC) is a common primary tumor[9, 10]. With the development of diagnostic imaging and advanced treatments in recent years, clinicians have adopted radical treatment strategies, such as surgical resection, liver transplantation, and radiofrequency ablation therapy. When used as initial treatments, curative techniques are only applicable to a small number of patients with HCC. Total cure for HCC is difficult to achieve because of high recurrence rates caused by multicentric carcinogenesis and intrahepatic metastasis. Hepatic apoptosis is regulated by autophagic activity. The complex interplay between hepatic autophagy and apoptosis determines the degree of hepatic apoptosis and the progression of liver disease. The autophagic pathway may be a novel therapeutic target for liver disease[7]. Therefore, scholars must screen and develop chemical compounds that can effectively inhibit HCC through the autophagic pathway to benefit public health.

The biological potential of indolo[2,3-*a*]carbazole derivatives has gained significant interest since the discovery of *staurosporine*, a glycosidic natural product from *Streptomyces staurosporeus*, in 1977. In 1986, this compound was found to be a non-specific nanomolar inhibitor of PKC *in vitro* and was regarded as a new platform for the design of potent, non-toxic, and selective antiproliferative agents[11, 12]. Bisindolylmaleimides, a series of derivative compounds, have received considerable attention in clinical trials, and they exhibit potential as anti-cancer drugs[13]. In the current study, BMA-155 exhibited distinct inhibitory activity in HepG-2 cells *in vitro* and *in vivo*. BMA-155 is a new derivative chemically synthesized from indole. Bisindolylmaleimides, such as arcyriarubin A, arcyriaflavin A, and staurosporine, can be dissolved in organic solvents (*eg*, DMSO)[14]. However, BMA-155 was easily salifiable to form BMA-155Cl, which could be dissolved in PBS; hence, BMA-155 has important potential for clinical applications.

We speculate that BMA-155Cl-induced autophagy and apoptosis exhibit broad spectrum effects. BMA-155Cl induces protective autophagy followed by apoptosis, and this action is associated with the NF-κB p65 signaling pathway in HepG-2 cells *in vitro* and *in vivo*.

Materials and methods
Materials
BMA-155 and its hydrochloride, BMA-155Cl, were synthesized by Zhu's group and identified by ESI-MS, ^{1}H and ^{13}C NMR data (Figure 1). BMA-155Cl was readily prepared by treating BMA-155 with HCl/ethyl acetate (3 mol/L). The purified BMA-155Cl (over 99% pure) was dissolved in dimethyl sulfoxide (DMSO, AppliChem, Germany) and diluted according to experimental requirements *in vitro* (the final concentration of DMSO was 4 µL/mL). 3-(4,5-Dimethylthiazol-2-yl)-2,5-di-
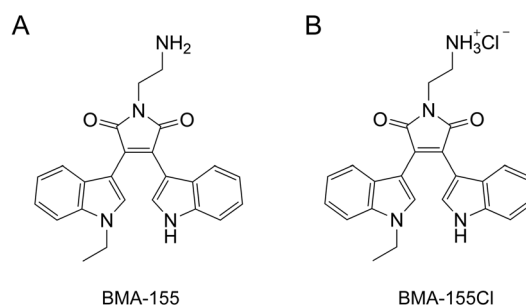

Figure 1. The chemical structure of BMA-155 (A) and BMA-155Cl (B).

phenyltetrazolium bromide (MTT), 3-methyladenine (3-MA, 5 mmol/L), monodansylcadaverine (MDS, 0.05 mmol/L), and 4′,6-diamidino-2-phenylindole (DAPI) were purchased from Sigma Co, USA. An Annexin V-FITC Apoptosis Detection Kit was obtained from BD Biosciences, USA. NF-κB p65 and IκB antibodies were purchased from Cell Signaling Technology (CST, USA). Anti-Bcl-2[E17] (ab32124) antibody, anti-Bax[E63] (ab32503) antibody, anti-p53[SP5] (ab16665) antibody and anti-p53[S6] (ab194731) antibody were purchased from Abcam® (USA). LC3B (SC-134226) and Beclin-1 (SC-10086) were obtained from Santa Cruz Biotechnology, Inc, USA. These were all rabbit monoclonal antibodies. A mouse monoclonal anti-glyceraldehyde-3-phosphate dehydrogenase (GAPDH) antibody was acquired from Zhongshan Jinqiao Biotechnology (Beijing, China). The NF-κB p65 inhibitor (BAY 11-7082, 10 µmol/L) and lysosomal protease inhibitors (pepstatin A, 10 µg/mL) were purchased from Beyotime (Shanghai, China). All other chemicals used in the experiments were commercial reagent grade products.

Cell culture
Human HCC cell lines (HepG-2, SMMC-7721, and Plc-prf-5) and human normal hepatocyte cell lines (LX-2, HL7702) were purchased from the Shanghai Institute for Biological Sciences (SIBS), Chinese Academy of Sciences and cultured in RPMI-1640 medium (HyClone) containing 10% fetal bovine serum (FBS) supplemented with 100 units/mL penicillin and 100 µg/mL streptomycin at 37 °C in a humidified atmosphere of 5% CO_2.

MTT assay
The cytotoxicity of BMA-155Cl was evaluated with MTT assays[2]. Cells (HepG-2, SMMC-7721, Plc-prf-5, LX-2, and HL7702) were seeded in 96-well plates (4×10^3–5×10^3 cells per well) overnight. After 24 h of incubation, cells were treated with or without 3-MA (5 mmol/L per well) 1 h prior to the administration of BMA-155Cl for the indicated time periods. To each well, 12 µL of MTT (5 mg/mL) was added, and then, cells were incubated at 37 °C for 4 h. The medium with MTT was removed, and 150 µL/well DMSO was added to dissolve the formed purple formazan crystals. Cell viability was assessed by recording the absorbance at 570 nm with a microplate reader (Bio-Rad 680). The cell inhibition ratio was cal-

culated as follows: cell inhibition ratio (%)=[1–(OD_{570}sample-OD_{570}blank)]/(OD_{570}control–OD_{570}blank) ×100.

Observation of morphological changes

Briefly, 5×10^4 cells/well (HepG-2, HL7702, and Plc-prf-5) were seeded in six-well culture plates. HepG-2 cells were incubated with or without 10 μmol/L BMA-155Cl for the indicated time periods (12 and 24 h). HL7702 cells were incubated with 10 and 20 μmol/L BMA-155Cl for 24 h. Plc-prf-5 cells were incubated with 5 and 10 μmol/L BMA-155Cl for 24 h. Cellular morphology was observed with a phase-contrast microscope (Nikon, TI-SR, Japan).

Transmission electron microscopy (TEM)

HepG-2 cells were treated or not treated with 10 μmol/L BMA-155Cl for the specified time periods. The cells were harvested with a cell scraper, centrifuged, fixed with 3% glutaraldehyde for 1 h at room temperature, and centrifuged again. Post-fixation, cells were treated with 0.15 mol/L phosphate buffer containing 3% osmium tetroxide for 1 h, followed by rapid wash in the same buffer. The specimens were dehydrated with alcohol–water solutions of varying concentrations and 100% propylene oxide. The specimens were then embedded with a 1:1 mixture of propylene oxide:araldite (*v/v*) for 1 h, followed by 1: 3 mixtures overnight at room temperature. Polymerization was induced at 60 °C for 3–4 d after treatment in undiluted resin for 1 h. Sections stained with 1% toluidine blue were placed on copper grids and observed with a transmission electron microscope (JEM-1200EX, Japan) at 60 kV.

Analysis of MDC staining

HepG-2 cells (2×10^4 cells/well) were seeded into 24-well plates with round 12-mm-diameter glass cover slips. After 24 h of incubation, the cells were treated with or without 3-MA (5 mmol/L per well) 1 h prior to administration of BMA-155Cl for 24 h. The cells were incubated in 0.05 mmol/L monodansylcadaverine (MDC) at 37 °C for 1 h. Coverslips containing cells were then mounted on microscope slides using mounting medium (PBS: glycerol=1:1). Changes in fluorescence were observed with confocal microscopy (ZEISS, LSM700, Germany). MDC staining was used to confirm the abundance of autophagic vacuoles in cells. The MDC-positive ratio was calculated by the following formula[15]: MDC-positive ratio (%)=[MDC-positive cell counts/100 cells]×100.

Cells with the same treatment were analyzed by flow cytometry. Cellular fluorescence was determined to estimate MDC intensity, and the results were analyzed with WinMDI 2.9 software.

GFP-LC3 localization observed with confocal microscopy

GFP-LC3 U87 cells (2×10^4 cells/well) were seeded into round 12-mm-diameter glass cover slips in 24-well plates. After 24 h of incubation, the cells were treated with or without 3-MA (5 mmol/L/well) 1 h prior to the administration of BMA-155Cl for 24 h. Then, cells were stained with 1 μg/mL DAPI for 10 min at room temperature. After washing three times with PBS-TX, coverslips containing cells were mounted on microscope slides and analyzed by confocal microscopy (ZEISS, LSM700, Germany).

Apoptotic bodies stained with DAPI observed using confocal microscopy

HepG-2 cells (2×10^4 cells/well) were seeded into round 12-mm-diameter glass cover slips in 24-well plates. After 24 h of incubation, the cells were treated with or without 3-MA (5 mmol/L per well) 1 h prior to administration of BMA-155Cl for 24 h. Cells were stained with 1 μg/mL DAPI for 10 min at room temperature. After washing three times with PBS-TX, coverslips containing cells were mounted on microscope slides and analyzed using confocal microscopy (ZEISS, LSM700, Germany). Cell viability (%)=[1–(DAPI positive cell counts of experimental group/DAPI positive cell counts of control)]×100.

Flow cytometric analysis of apoptosis and autophagy

HepG-2 cells (5×10^4 cells/well) were seeded in six-well culture plates. After 24 h of incubation, the cells were treated with or without 3-MA (5 mmol/L per well) 1 h prior to administration of BMA-155Cl for 24 h. A BD Pharmingen™ Annexin V: FITC Apoptosis Detection Kit was used for apoptosis evaluation. The cells were washed with ice-cold PBS and trypsinized. Each cell sample was transferred to individual tubes and centrifuged at 200×*g* for 5 min. The supernatant was removed, and the cells were resuspended in 400 μL of binding buffer. The cells were incubated at room temperature in the dark for 15 min with 5 μL of Annexin V-FITC, and then, 5 μL (50 mg/L) of propidium iodide (PI) was added, and the cells were incubated for another 5 min.

To assess autophagy, cells were incubated with 0.05 mmol/L monodansylcadaverine (MDC) at 37 °C for 1 h. According to the manufacturer's instructions, the samples were analyzed by flow cytometry (Becton Dickinson, USA). The apoptotic data were post-processed with WinMDI 2.9 analysis software.

RNA extraction and relative quantification using real-time PCR

Total RNA was extracted using an RNAEasy kit according to the manufacturer's instructions (Bioecon Biotec Co Ltd, China). RNA purity was checked by measuring the $OD_{260/280}$ of RNA samples (>1.8). cDNA was synthesized through reverse transcription using M-MLV reverse transcriptase and oligo(dT) primer. The gene expression levels of NF-κB p65, p53, Beclin-1, and Bax were detected by real-time PCR. PCR amplification was performed in an eight-tube strip format (Axygen, Union City, CA) in triplicate. Each reaction contained 1×SYBR Green PCR Master mix, 1 μmol/L forward and reverse primers, and 1 μL of template cDNA to obtain a final volume of 20 μL, and PCR was performed using a Mastercycler ep realplex apparatus (Eppendorf, Germany). The following primers were used: primers based on the NF-κB p65 gene (forward: 5′-GAGGACTGCTGCTACGTCAC-3′ and reverse: 5′-ACCAGGTTCAGGTTCAGCTC-3′), Beclin-1 gene (forward: 5′-CCACAGCCCAGGCGAAACCA-3′ and

reverse: 5′-CCGCCATCAGATGCCTCCC-3′), p53 gene (forward: 5′-TAACAGTTCCTGCATGGGCGGC-3′ and reverse: 5′-AGGACAGGCACAAACACGCACC-3′), and the Bax gene (forward: 5′-TCAACTGGGGGCCGGGTTGTC-3′ and reverse: 5′-CCTGGTCTTGGATCCAGCC-3′). Evaluation of the GAPDH expression was utilized as a control for RNA amount and was conducted with a primer (forward: 5′-GACGGCCG-CATCTTCTTGT-3′ and reverse: 5′-CACACCGACCTTCAC-CATTTT-3′)[16-18]. Amplification was performed for 45 cycles of sequential denaturation (95 °C, 2 min); annealing (60 °C, 15 s); and extension (72 °C, 20 s). A Mastercycler ep realplex was used to obtain real-time PCR assay data. Each fluorescent reporter signal was measured against the internal reference dye signal to normalize the non-PCR-related fluorescence fluctuations among the wells. All samples were studied in independent triplicate experiments. All primers were synthesized by Sangon Co, Ltd (Shanghai, China).

Isolation of nuclear and cytosolic fractions and Western blot analysis

Cells were separated into two fractions, nuclear and cytosolic, using a Nuclear and Cytoplasmic Protein Extraction Kit (Beyotime Inst, Haimen, China). The treated cells were washed with ice-cold PBS and suspended in 200 µL of Reagent A containing 1 mmol/L PMSF. The cells were vortexed for 5 s, incubated on ice for 15 min, and 10 µL of Reagent B was added. The above procedure was repeated. The precipitate contained the nuclei separated from the cytosolic extracts by centrifugation (16 000×g, 5 min at 4 °C). The supernatant liquid was the cytosolic fraction. The nuclear pellets were resuspended in nuclear protein reagent for 30 min at 4 °C under agitation. The nuclear proteins remained in the supernatants after centrifugation (16 000×g, 10 min at 4 °C). The cells were lysed with whole-cell extraction buffer [50 mmol/L Tris-HCl, 2% sodium dodecyl sulfate (SDS), 10% glycerol, 100 mmol/L DTT (*DL*-dithiothreitol)] to obtain whole-cell proteins for western blot analyses. The samples were subjected to 8%–12% SDS-polyacrylamide gel electrophoresis and transferred to nitrocellulose membranes. The membranes were washed with distilled water and blocked with 5% non-fat milk in TBS-T buffer (10 mmol/L Tris-HCl, 150 mmol/L NaCl, and 0.05% [*v/v*] Tween-20; pH 7.8) for at least 1 h at room temperature. The membranes were incubated in a solution containing monoclonal antibodies specific for NF-κB p65, IκB, LC3B, Beclin-1, p53, p-p53, Bax, Bcl-2, and GAPDH overnight at 4 °C. The membranes were incubated with secondary biotin-conjugated goat anti-mouse IgG or anti-rabbit IgG (diluted 1:1000; Santa Cruz Biotechnology, Inc, USA). Protein expression was quantified by densitometry using Alpha View software[2].

In vivo xenograft study

Balb/c athymic (nu+/nu+) male mice, 5–6 weeks old, were purchased from the Animal Center of China Academy of Medical Sciences (Beijing, China). All animal experiments were performed in accordance with the institutional guidelines of the Animal Care and Use Committee at Shandong University.

Briefly, 2×10^6 HepG-2 cells in 0.1 mL of normal saline (NS) were subcutaneously (sc) injected into the right armpit of one mouse to establish an HCC xenograft model. After 3 weeks, the rapidly proliferating tumor was cut into 1.5-mm-thick pieces and subcutaneously implanted into the right armpit of nude mice with a puncture needle. Tumor sizes were measured with a caliper. When the tumors grew to approximately 100 mm^3, the tumor-bearing mice were randomly separated into four groups (*n*=6/group): vehicle (NS), vincristine (0.4 mg/kg), and BMA-155Cl (10 and 20 mg/kg). All drugs and vehicle were intraperitoneally (ip) injected into the mice once every 3 d, for a total of 18 d. The tumor volumes and the body weights of the mice were measured every 3 d. Inhibition of cancer growth was defined as the ratios of the weight and volume of experimental tumors to those of the vehicle control tumors. At the end of the experiments, the mice were euthanized, and tumor tissues were excised. The tissues were homogenized to extract proteins for Western blot analysis and prepare slices for H&E staining and immunohistochemistry (IHC).

IHC and H&E staining

IHC and HE staining were performed by Shandong Academy of Medical Sciences. IHC was performed using an SP-9000 Histostain™-Plus Kit (Beijing Zhongshan Golden Bridge Biotechnology Co, Ltd) according to the manufacturer's instructions. LC3B, Beclin-1, NF-κB p65, and IκB antibodies were diluted at 1:100. HE staining was conducted using a DAB Kit (Beijing Zhongshan Golden Bridge Biotechnology Co, Ltd) according to the manufacturer's instructions. Images were captured with a fluorescence microscope (Nikon, TI-SR, Japan) in brightfield. Staining intensity was scored as 0 (negative), 1 (weak), 2 (medium), or 3 (strong). The extent of staining was scored as 0 (0%), 1 (1%–25%), 2 (26%–50%), 3 (51%–75%), or 4 (76%–100%) according to the percentage of the positively stained area in the entire carcinoma area[19, 20]. The sum of the intensity and extent score was considered the final staining score for NF-κB p65, IκB, LC3B, Beclin-1, Bax, and Bcl-2.

Statistical analysis

All experiments were performed at least three times. Statistical analysis was performed with analysis of variance (ANOVA), followed by Tukey's *t*-test. *P*-values <0.05 were considered statistically significant.

Results

Antitumor effect of BMA-155Cl *in vitro* and *in vivo*

We used an MTT colorimetric assay to determine the cytotoxic effect of BMA-155Cl on human hepatocarcinoma and normal liver cells. Three human hepatocarcinoma cell lines (HepG-2, SMMC-7721, and Plc-prf-5), a human hepatic stellate cell line, LX-2, and a normal HL7702 cell line were treated with BMA-155Cl for 24, 48, and 72 h. As shown in Table 1, BMA-155Cl inhibited the growth of human hepatocarcinoma cell lines and was less cytotoxic to the normal cell lines than to the cancer cell lines. The IC$_{50}$ values of BMA-155Cl in HepG-2 cells were

16.62±1.34, 12.21±0.83, and 8.44±1.82 μmol/L at 24, 48, and 72 h, respectively (Table 1). Further experiments showed that BMA-155Cl dose- and time-dependently inhibited the proliferation of HepG-2 cells (Figure 2A).

The anti-tumor effect of BMA-155Cl was further evaluated *in vivo* in nude mice bearing HepG-2 xenografts. The tumor volumes in the experimental groups grew more slowly than in the vehicle control group (Figure 2B). The body weight significantly decreased in the experimental groups, especially in the vincristine-treated group (Figure 2C). After treatment with 10 and 20 mg/kg BMA-155Cl, HepG-2 xenografts exhibited a 31.5% and 51.0% reduction in weight, respectively, and a 34.6% and 59.4% reduction in tumor volume, respectively. Vincristine (0.4 mg/kg) exhibited superior inhibitory activity on HepG-2 xenografts (with tumor weight inhibition of 63.6% and tumor volume inhibition of 77.9%) (Table 2). BMA-155Cl injection was generally well tolerated by mice with no significant loss of body weight compared with the vincristine-treated group (Figure 2C). HE staining showed necrosis of the tumor tissue in the group injected with 20 mg/kg BMA-155Cl, whereas tumors in the vehicle control group displayed abundant blood vessels and vigorous growth (Figure 2D).

BMA-155Cl induces autophagy *in vitro*

Autophagy and apoptosis were observed in BMA-155Cl-treated cells using an inverted optical microscope (Figure 3A).

Vacuoles induced by BMA-155Cl formed as early as 6 h post-treatment. The number and size of the vacuoles increased progressively with prolonged treatment. After 12 h of incubation with 10 μmol/LBMA-155Cl, the cells exhibited cytoplasmic vacuolization (indicated by blank arrow, as shown in Figure 3A; 12 h). By contrast, prolonged BMA-155Cl treatment up to 24 h resulted in apoptosis, which was characterized by nuclear condensation and segregation (indicated by white arrow, as shown in Figure 3A; 24 h), without increasing the number of autophagic vacuoles.

The ultrastructural details in BMA-155Cl-treated cells were further examined by TEM. Treatment with BMA-155Cl resulted in the appearance of numerous vacuoles in HepG-2 cells in contrast to control cells (Figure 3B). At 15 h, we clearly observed double membrane-bound vacuoles containing organelles and cellular fragments, indicating that they were autolysosomes[2]. Extending the treatment with BMA-155Cl to 24 h resulted in apoptotic cell death, characterized by nuclear condensation and segregation (indicated by white arrow, as shown in Figure 3B; 24 h) in contrast to autophagic cells.

In addition, using flow cytometry, we confirmed that BMA-155Cl induced autophagy. As shown in Figure 3C and 3D, BMA-155Cl increased the number of autolysosomes stained with MDC in a dose- and time-dependent manner in HepG-2 cells. The level of autophagy was highest at 10 μmol/L and 15 h, indicating that 10 μmol/L BMA-155Cl induced the most

Table 1. Cytotoxicity of BMA-155Cl in various human hepatic cell lines. Data are expressed as the mean±SD of three independent experiments.

Cell lines	IC$_{50}$ (μmol/L)			
	72 h	48 h	24 h	Dox (48 h)
HepG-2	8.44±1.82	12.21±0.83	16.62±1.34	0.58±0.18
SMMC-7721	8.93±1.25	12.58±1.84	20.62±1.89	0.6±0.076
LX-2	13.66±1.15	20±3.38	29.23±1.44	0.91±0.22
Plc-prf-5	16.35±3.39	28.57±4.5	32.55±1.0	0.59±0.079
HL7702	36.17±3.16	>40	>40	1.12±0.2

The effects of BMA-155Cl on various human hepatocellular carcinoma cells (HepG-2, SMMC-7721, Plc-prf-5) and normal hepatic cells (LX-2, HL7702) were examined by MTT assay. The cells were treated with various concentrations of BMA-155Cl for 72, 48, and 24 h. The IC$_{50}$ values of BMA-155Cl were then calculated.

Table 2. The inhibitory effects of BMA-155Cl on the growth of HepG-2 xenografts in nude mice.

Drugs and dosage	Mice number (*n*)	Body weight (g) (initial/end)	Tumor weight (g) (mean±SD)	Tumor weight inhibition (%)	Tumor volume (mm^3) (initial/end)	Tumor volume inhibition (%)
Vehicle	6	22.3±1.0/21.9±1.8	1.43±0.62	–	53.8±17.34/465.9±40.6	–
Vincristine (0.4 mg/kg)	6	21.8±1.6/17.1±1.7**	0.52±0.37*	63.6	61.2±16.3/152.4±21.8*	77.9
BMA-155Cl (10 mg/kg)	6	21.9±2.1/22.7±2.5	0.98±0.33*	31.5	50.0±18.0/319.7±26.0*	34.6
BMA-155Cl (20 mg/kg)	6	22.1±1.4/20.2±1.8	0.70±0.24*	51.0	51.1±16.3/218.5±38.8*	59.4

Established tumors were treated with BMA-155Cl by injection intraperitoneally. Body weight and tumor volume were examined before and after drug administration. Tumor weight was measured after mice were sacrificed. Tumor weight inhibition (%)=(1–tumor weight of experimental group/tumor weight of vehicle group)×100%; Tumor volume inhibition (%)=(1–tumor growth volume of experimental group/tumor growth volume of vehicle group)×100%. Note: tumor growth volume=tumor volume (end)–tumor volume (initial). *$P<0.05$, **$P<0.01$ *vs* vehicle.
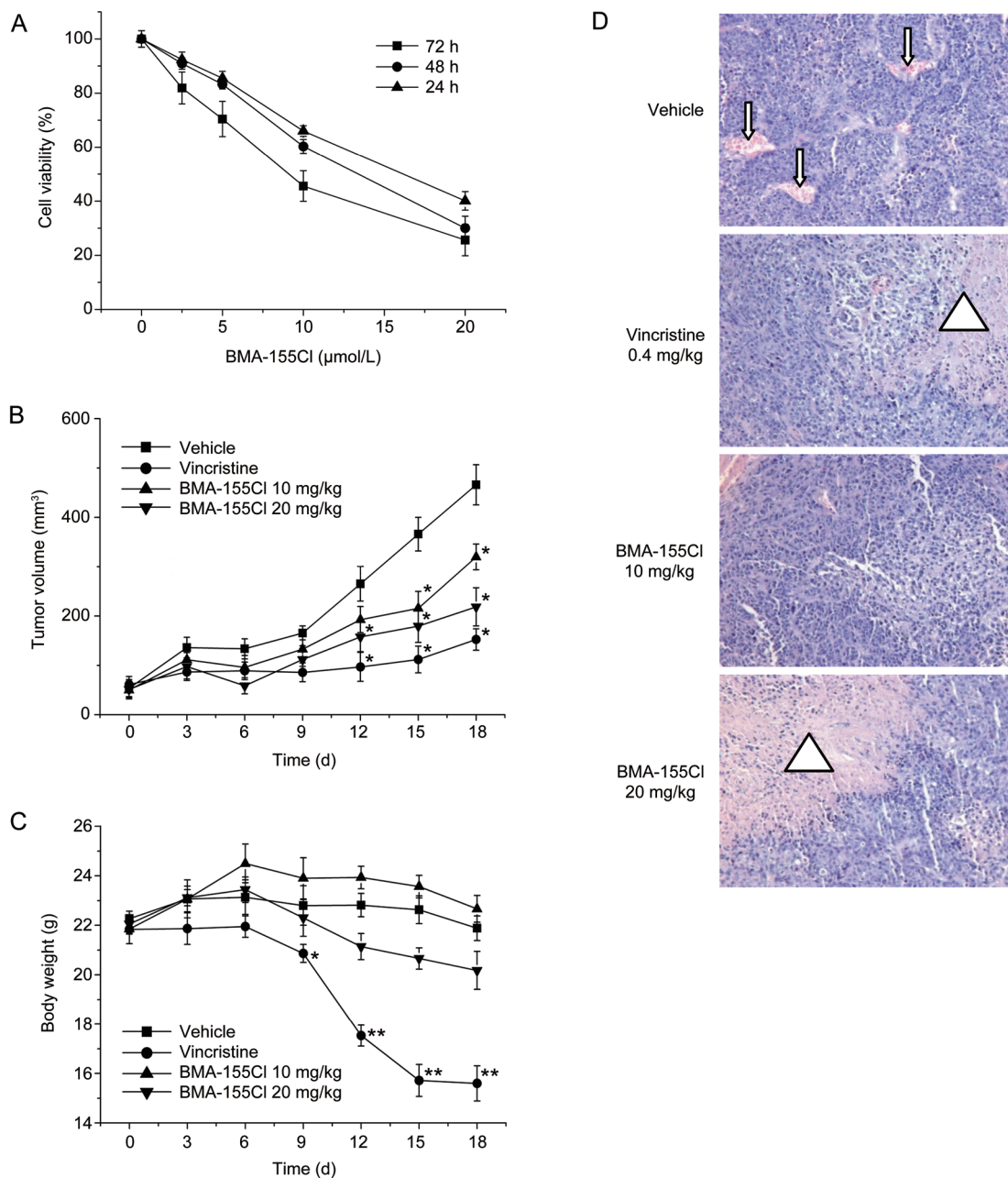
Figure 2. BMA-155Cl's antitumor effect *in vitro* and *in vivo*. (A) HepG-2 cells were treated with 2.5–20 µmol/L BMA-155Cl respectively for 24–72 h. Cells viability was estimated by MTT assay. Data were obtained from three independent experiments and presented as the mean±SD. BMA-155Cl inhibited the growth of tumor volume (B) and body weight (C) *in vivo*. Data were presented as mean±SD. *n*=6. (D) BMA-155Cl induced the necrosis of the tumor tissue after H&E staining. The blood vessels were presented as red regulated pattern in vehicle group (pointed by the arrow), whereas the necrosis zones were presented as patches of red in vincristine and BMA-155Cl groups (pointed by the triangle). Magnification ×200. $^{*}P<0.05$, $^{**}P<0.01$ *vs* vehicle.

evident autophagic phenomena after 15 h of treatment.

To confirm the broad spectrum effect of BMA-155Cl on autophagy induction, we also observed HL7702, Plc-prf-5 and GFP-LC3 U87 cells after treatment with BMA-155Cl for 24 h. BMA-155Cl induced autophagy in HL7702 and Plc-prf-5 cells (Figure 3E) and the recruitment of GFP-LC3 during autophagosome formation (Figure 5H).

BMA-155Cl induces apoptosis in HepG-2 cells *in vitro*

Flow cytometry analysis showed that treatment with 5, 10, and 20 µmol/L BMA-155Cl for 24 h increased the number of apoptotic cells by 24.81%, 37.35%, and 50.72%, respectively (Figure 4A). BMA-155Cl time-dependently induced apoptosis in HepG-2 cells. After treatment with BMA-155Cl for 12, 24, and 48 h, the apoptotic ratios were 28.09%, 34.04%, and 48.60%, respectively (Figure 4B).
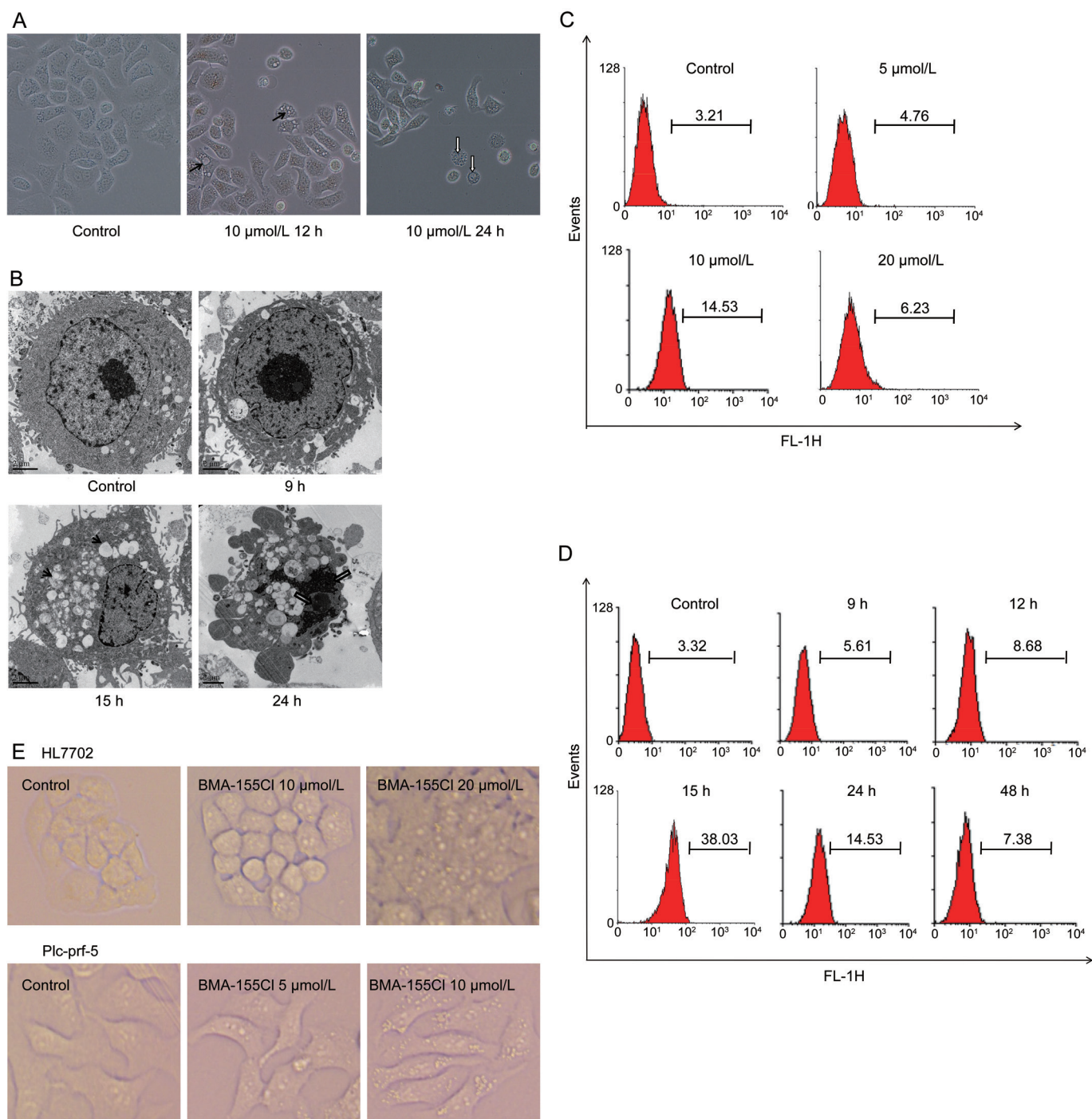
Figure 3. Induction of autophagy by BMA-155Cl in HepG-2 cells. The morphological changes of HepG-2 cells treated with 10 μmol/L BMA-155Cl were observed using phased-contrast microscopy (A) and transmission electron microscope (B, the bar was 2 μm). Autophagic vacuoles were shown as the black arrows at 12 h and 15 h, whereas the apoptosis characterized by nuclear condensation and segregation were shown as the white arrows showed at 24 h. MDC quantitative analysis of HepG-2 cells treated with 0–20 μmol/L BMA-155Cl for 24 h (C) and with 10 μmol/L BMA-155Cl for appointed time (D). (E) The cells (HL7702 and Plc-prf-5) morphological changes were observed using phased-contrast microscopy after being treated with BMA-155Cl for 24 h. Magnification ×40.

Inhibition of autophagy by 3-MA potentiated BMA-155Cl-induced apoptotic cell death

The interconnection between BMA-155Cl-induced autophagy and apoptosis was further investigated using the autophagy inhibitor 3-MA. As shown in Figure 5A, the IC$_{50}$ value of BMA-155Cl at 24 h decreased from 16.62±1.34 μmol/L to 9.5±1.1 μmol/L in the presence of 5 mmol/L 3-MA (cells treated with 5 mmol/L 3-MA alone showed less toxicity, with
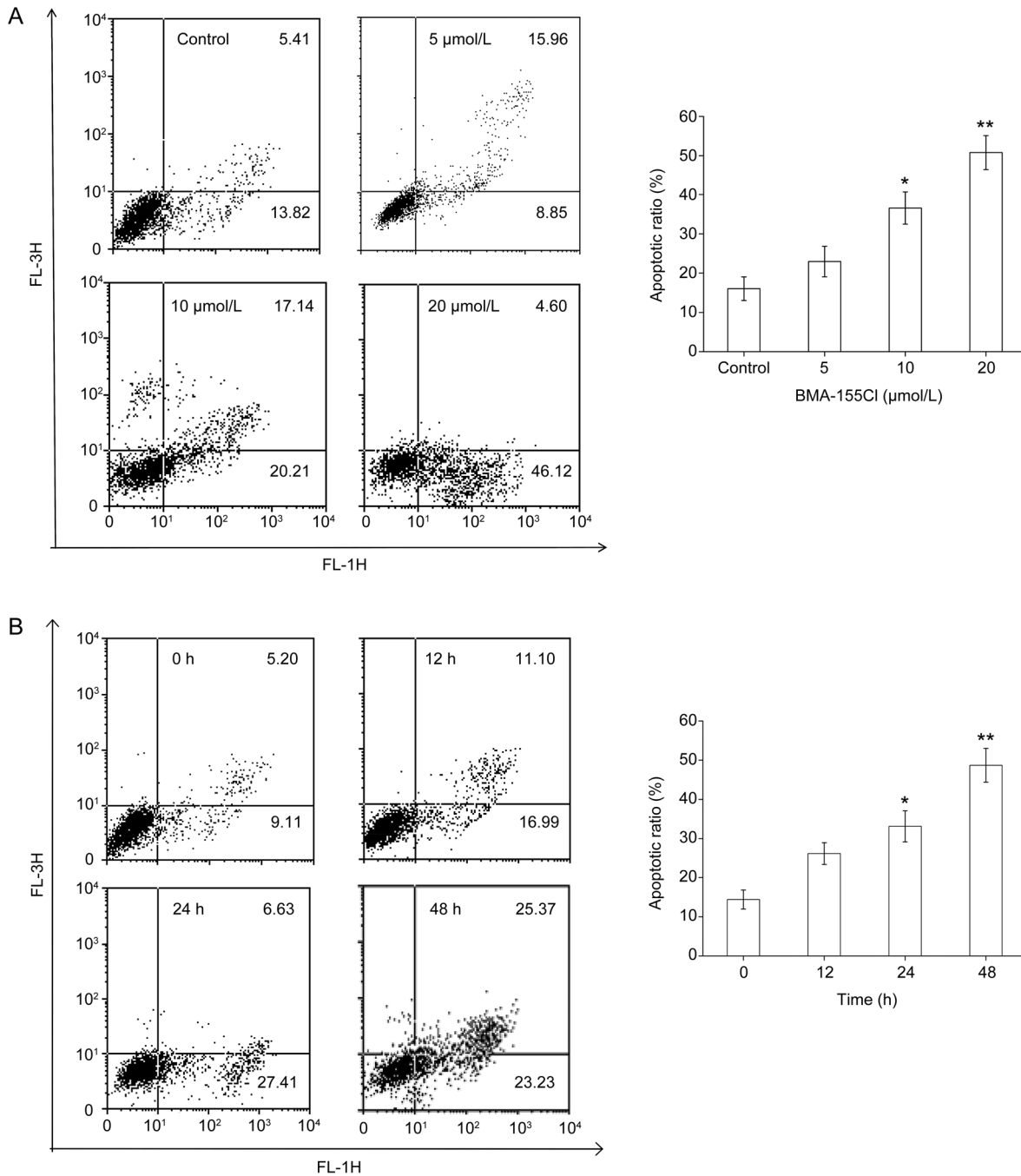
Figure 4. BMA-155Cl induces HepG-2 cells apoptosis *in vitro*. The apoptotic ratio was measured by flow cytometry. The apoptotic ratio increased in a dose-dependent manner (A, treated for 24 h) and in a time-dependent manner (B, treated with 10 µmol/L BMA-155Cl). The corresponding histograms were presented on the right side, respectively. The data were expressed as the mean±SD of triplicate experiments. $^*P<0.05$, $^{**}P<0.01$ *vs* control (Note: We set LR+UR as apoptosis rate).

cell viability of approximately 95.33%±4.3%). Flow cytometry analysis indicated that 10 µmol/L BMA-155Cl induced apoptosis, with an apoptotic ratio of 34.98%. By contrast, 5 mmol/L 3-MA potentiated the apoptosis of cells induced by 10 µmol/L BMA-155Cl by increasing the apoptotic ratio to 58.47% (Figures 5B and C). In addition, MDC staining showed that 3-MA suppressed the formation of autophagosomes at the early stages of autophagy to exert an autophagy-inhibiting effect (Figure 5D). The MDC-positive ratio decreased from 58.76% (group treated with 10 µmol/L BMA-155Cl alone) to 33.58% (group treated with 10 µmol/L BMA-155Cl in the presence of 5 mmol/L 3-MA) (Figure 5F). We used DAPI staining to observe the formation of BMA-155Cl-induced apoptotic bodies. BMA-155Cl dose-dependently induced apoptosis
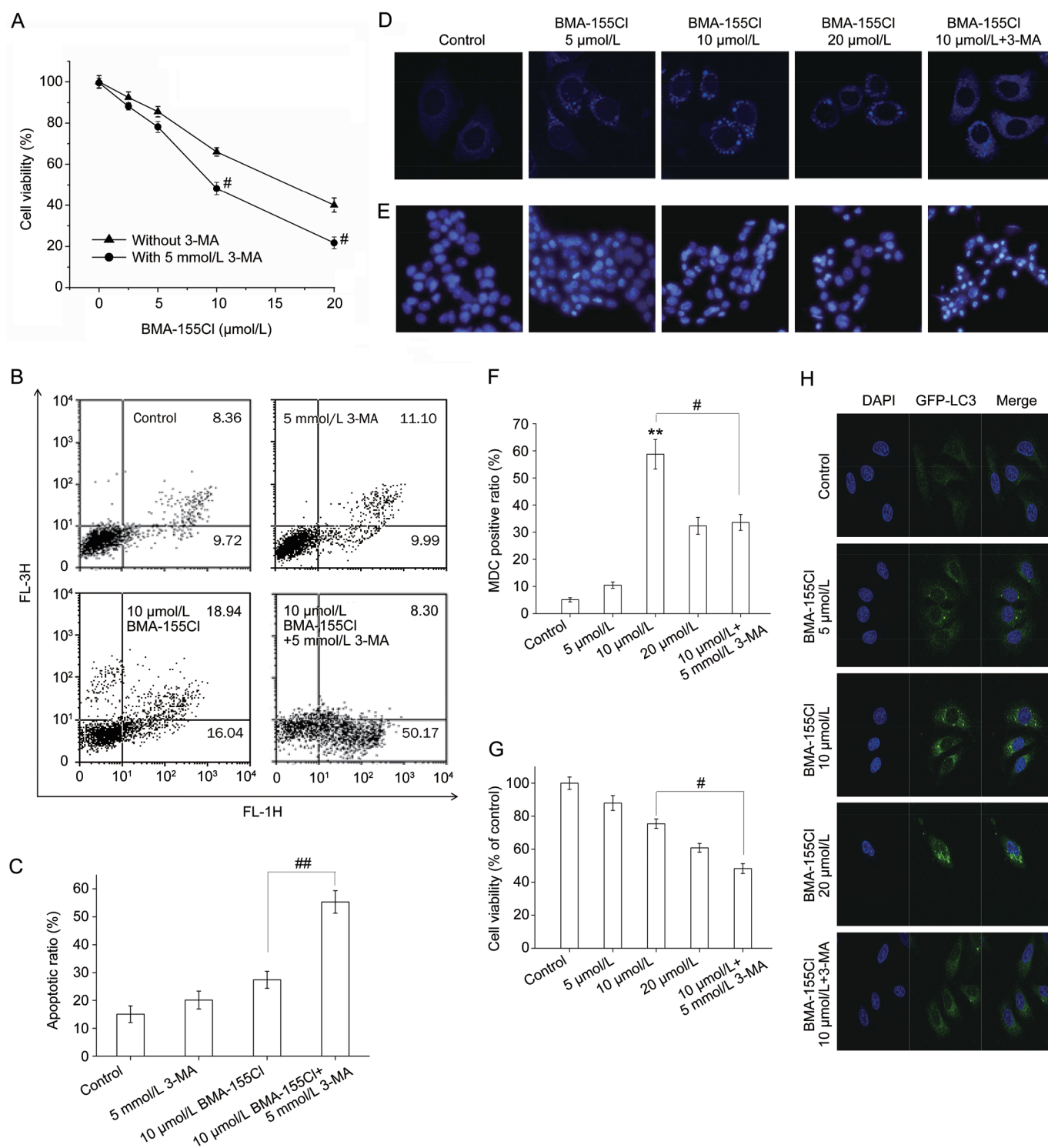
Figure 5. Inhibition of autophagy by 3-MA potentiates BMA-155Cl's pro-apoptotic effect. HepG-2 cells were treated with various concentrations of BMA-155Cl (5–20 μmol/L) for 24 h in the absence or presence of 3-MA (5 mmol/L, pretreated for 1 h). The cell viability ratio (A) and the apoptotic ratio (B) were measured by MTT and flow cytometry. The MDC staining (D) and DAPI staining (E) assay were performed by confocal microscopy. The corresponding quantified histograms of B, D and E are presented as C, F and G, respectively. (H) BMA-155Cl induced accumulation of GFP-LC3 puncta in U87 cells in a dose-dependent manner within 24 h. Magnification ×40. All data were expressed as the mean±SD of triplicate experiments. [**]$P<0.01$ *vs* control. [#]$P<0.05$, [##]$P<0.01$ vs BMA-155Cl 10 μmol/L.

(Figure 5E). Pretreatment with 3-MA for 1 h enhanced BMA-155Cl-induced apoptosis compared with the BMA-155Cl treatment alone (Figure 5E). The cell viability decreased from 75.43% (group treated with 10 μmol/L BMA-155Cl alone)

to 48.27% (group treated with 10 µmol/L BMA-155Cl in the presence of 5 mmol/L 3-MA) (Figure 5G). These results show that 3-MA inhibited BMA-155Cl-mediated autophagy but sensitized HepG-2 cells to the cytotoxic and apoptotic effects of BMA-155Cl.

BMA-155Cl modulates the gene expression of NF-κB, p53, Beclin-1, and Bax

To further analyze the mechanism of BMA-155Cl-induced autophagy followed by apoptosis in HepG-2 cells, we evaluated the effect of BMA-155Cl on the mRNA levels of NF-κB, Beclin-1, p53, and Bax through real-time quantitative RT-PCR analysis. The results showed that BMA-155Cl increased NF-κB, Beclin-1, p53, and Bax gene expression in a time-dependent manner (Figure 6A). Beclin-1 was activated prior to Bax, and the activation of NF-κB mRNA peaked as early as approximately 4 h. Hence, the NF-κB signaling pathway is involved in autophagic apoptosis in BMA-155Cl-treated HepG-2 cells. We predict that autophagy occurred prior to apoptosis.

BMA-155Cl modulates the expression of Beclin-1, LC3B, p53, p-p53, Bax, and Bcl-2 *in vitro*

We also tested the expression of Beclin-1, LC3B, p53, p-p53, Bax and Bcl-2 using a Western blot analysis (Figure 6B and C). Treatment with BMA-155Cl increased the protein expression of Beclin-1, LC3B, p53, p-p53, and Bax in HepG-2 cells but decreased the expression of Bcl-2, an important anti-apoptosis protein. Interestingly, treatment with 10 µmol/L BMA-155Cl for 24 h slightly decreased the LC3B expression and steadily increased the Bax expression compared with treatment for 12 h. Hence, BMA-155Cl induced protective autophagy followed by apoptosis (Figure 6C). Interpretation of the results of LC3 immunoblotting is problematic because LC3B itself is degraded by autophagy. To determine whether BMA-155Cl induced the formation of autophagy or suppressed the degradation of autophagy, we tested the expression of LC3B in samples in the presence and absence of pepstatin A (a lysosomal protease inhibitor, 10 µg/mL). Pretreatment with pepstatin A for 1 h enhanced the LC3B level compared with treatment with 10 µmol/L BMA-155Cl alone for 24 h (Figure 6D). Hence, BMA-155Cl induced the occurrence of autophagy.

BMA-155Cl modulates the expression of NF-κB p65 and IκB

NF-κB is an important transcription factor that regulates the synthesis and secretion of various cytokines and chemokines in response to immunological stimuli; as such, we examined the role of NF-κB in BMA-155Cl-induced autophagy and apoptosis in HepG-2 cells using a Western blot[21]. NF-κB p65 activation and deactivation are mediated by phosphorylation and degradation of IκB protein. The nuclear translocation of NF-κB p65 is an important characteristic of autophagy[22]. Our results showed that BMA-155Cl treatment dose-dependently enhanced NF-κB p65 expression but decreased IκB expression in the total protein extracts (Figure 6B). We also determined NF-κB p65 protein levels in different cellular fractions (*ie*, the nucleus and cytoplasm) with a Western blot analysis. Compared with the control, BMA-155Cl-induced HepG-2 cells exhibited considerably increased expression of NF-κB p65 in the nucleus but decreased expression in the cytoplasm (Figure 6F).

Inhibition of NF-κB suppresses the activation of p53, p-p53, LC3B, and Bax in BMA-155Cl-induced apoptotic cell death

To understand the mechanism of NF-κB p65 in BMA-155Cl-induced autophagy and apoptosis, we examined the expression levels of p53, p-p53, LC3B, Bax, and Bcl-2 in the absence or presence of 10 µmol/L BAY 11-7082 (a specific inhibitor of NF-κB p65). Treatment with 10 µmol/L BAY 11-7082 alone showed minimal cytotoxicity to HepG-2 cells, with cell viability of approximately 93.27%±2.2%. A decreased level of p53, p-p53, LC3B, and Bax and an increased level of Bcl-2 in the presence of 10 µmol/L BAY 11-7082 compared with BMA-155Cl treatment alone confirmed the involvement of NF-κB p65 in BMA-155Cl-induced autophagy and apoptosis in HepG-2 cells (Figure 6E).

BMA-155Cl regulates autophagy and apoptosis through the NF-κB p65 pathway *in vivo*

Finally, we tested the expression of Beclin-1, LC3B, NF-κB, IκB, Bax, and Bcl-2 after treatment with BMA-155Cl in HepG-2 xenografts using a Western blot (Figure 7A and 7B). BMA-155Cl increased the protein expression of Beclin-1, LC3B, NF-κB p65, and Bax and decreased the protein expression of Bcl-2 and IκB. IHC results also demonstrated similar expression levels of Beclin-1, LC3B, Bax, Bcl-2, NF-κB p65, and IκB in BMA-155Cl-treated HepG-2 xenografts; this finding significantly differed from that of the control (Figure 7C).

Discussion

Various bisindolylmaleimide derivatives have been synthesized to reduce the cytotoxicity and improve the anti-tumor activity of drugs for clinical applications[13, 23]. Despite the potent activity, most compounds have limited water solubility because of their hydrophobic nature, thereby restricting *in vivo* studies. Alkylation of the side chains of the indole nitrogen plays an important role in the anti-tumor activity of these compounds. In a preliminary screening, we found that treatments with BMA-155Cl for 24 h induced autophagy and the recruitment of GFP-LC3 in HL7702, Plc-prf-5, and GFP-LC3 U87 cells during autophagosome formation; this finding confirms the broad spectrum effect of BMA-155Cl on autophagy induction. This phenomenon was clearly observed in HepG-2 cells. Notably, BMA-155 is a new and easily salifiable bisindolylmaleimide compound with potential as a therapeutic drug *in vivo*. Thus, we chose HepG-2 cells for the experiments using BMA-155 salts (specifically, BMA-155Cl) *in vitro* and *in vivo*.

Apoptosis and autophagy are two different processes of programmed cell death (PCD). Apoptosis controls the intercellular steady state and the development of individual organisms[24]. The induction of autophagy, which is known
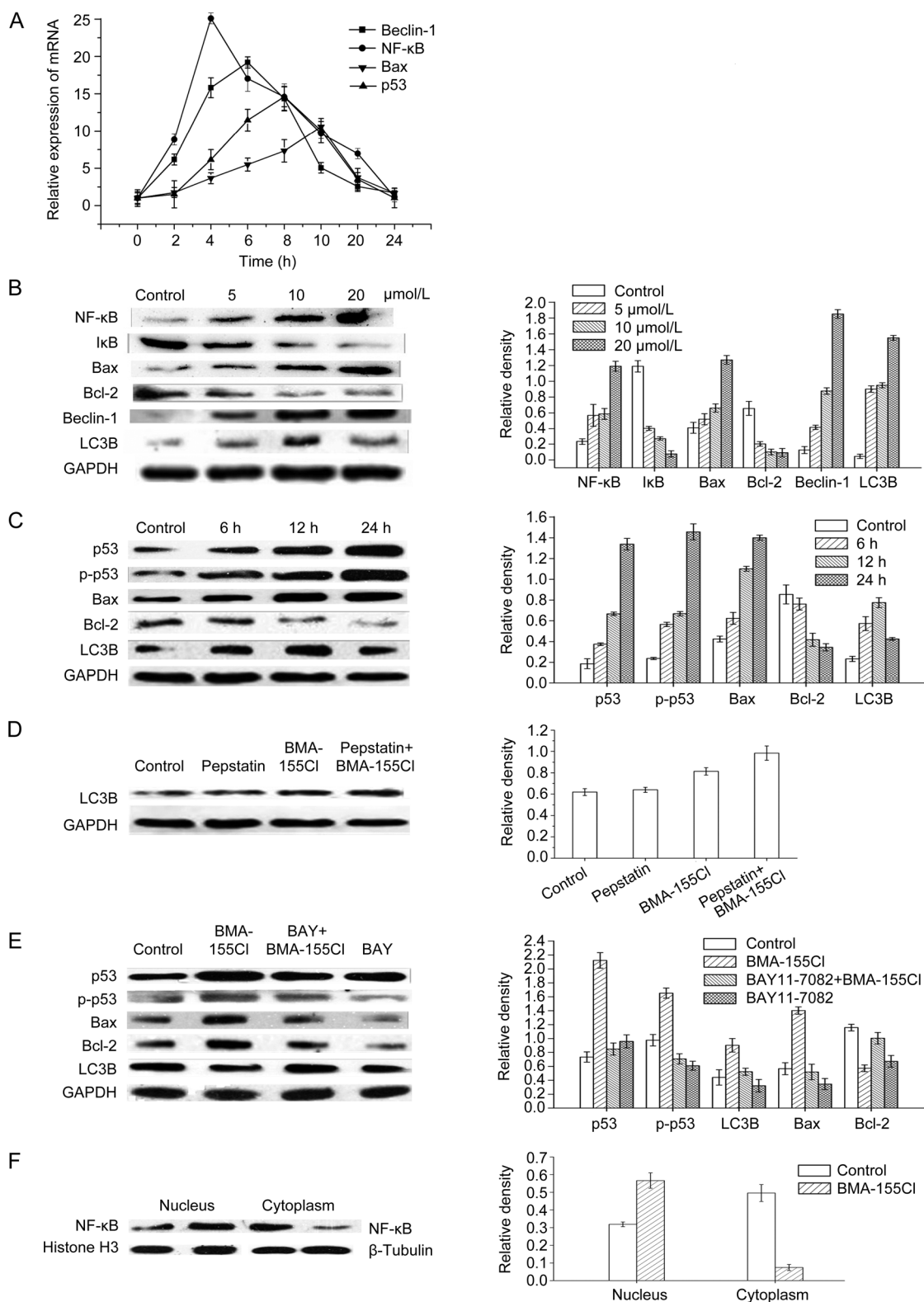
Figure 6. BMA-155Cl regulates autophagy and apoptosis through NF-κB p65 pathway *in vitro*. (A) Relative expressions of mRNA were determined by relative quantification real-time PCR. All mRNA levels were normalized to GAPDH mRNA levels. Western blot and its quantification results indicated that BMA-155Cl enhanced levels of NF-κB p65, Bax, Beclin-1, LC3B, p53, p-p53 proteins, whereas decreased the levels of IκB and Bcl-2 proteins in a dose-dependent manner (B) and in a time-dependent manner (C). (D) Pretreatment with pepstatin A (10 μg/mL) for 1 h enhanced LC3B level comparing with the 10 μmol/L BMA-155Cl treatment alone for 24 h. (E) The inhibition of NF-κB p65 (with BAY 11-7082) decreased the levels of p53, p-p53, LC3B, and Bax, whereas increased the levels of Bcl-2 in BMA-155Cl-treated cells. (F) The decreased NF-κB p65 levels in cytoplasm but not in nucleus and its corresponding histograms. All data were expressed as the mean±SD of triplicate independent experiments.
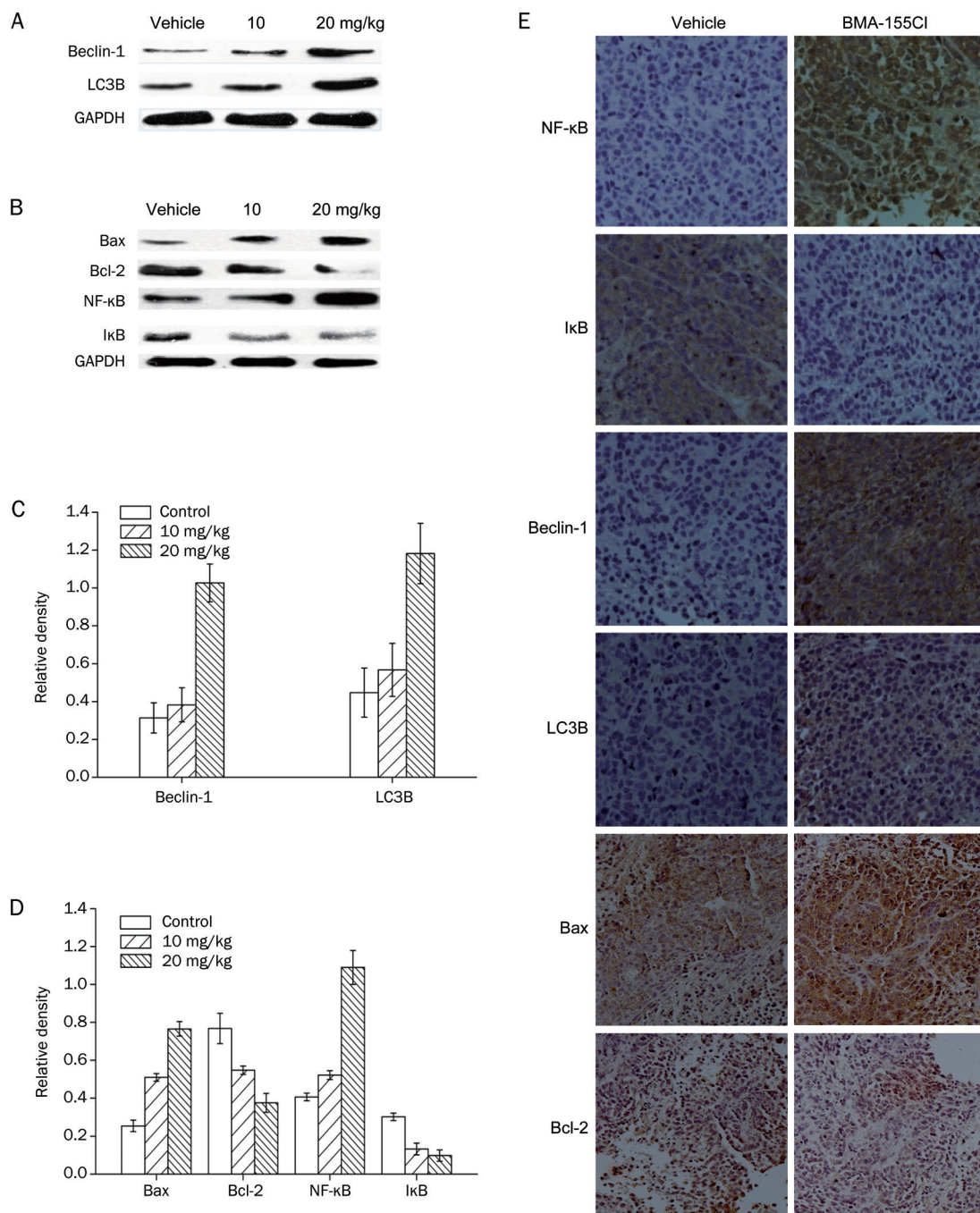
Figure 7. BMA-155Cl regulates autopahgy and apoptosis through NF-κB p65 pathway *in vivo*. Western blot and its quantification results indicated that BMA-155Cl enhanced levels of LC3B, Beclin-1, NF-κB, and Bax, whereas decreased the levels of IκB and Bcl-2 (A, B). The corresponding histograms quantified through densitometry were presented as C and D. The data were expressed as the mean±SD of triplicate independent experiments. (E) The expressions of NF-κB p65, IκB, Beclin-1, LC3B, Bax, and Bcl-2 in the tumor tissues were determined by immunohistochemical analysis. Magnification ×200.

to maintain cell survival under conditions of cellular stress, such as a shortage of nutrients, metabolic stress, and intracellular damage, is a common survival mechanism in eukaryotic cells[4]. Many reports have demonstrated that apoptosis and autophagy exhibit complex relationships, and many gene- and protein-controlled apoptosis pathways regulate autophagy.

In this study, autophagosomes markedly accumulated at the early stages of autophagy (at approximately 6 h) in BMA-155Cl-treated cells and peaked at approximately 15 h, as observed through TEM analysis. With MDC staining and observation using fluorescence microscopy and flow cytometry (FCM), we confirmed the autophagy activity, consis-

tent with the reports of previous studies. Prolonging BMA-155Cl treatment induced the occurrence of apoptosis *in vitro*. Quantitative analysis using Annexin V-FITC/PI staining indicated that the population of apoptotic cells increased after BMA-155Cl treatment. DAPI staining results revealed that BMA-155Cl-treated cells exhibited obvious apoptotic features, thereby confirming that BMA-155Cl induced apoptosis in HepG-2 cells. The effect of autophagy induced by BMA-155Cl was further confirmed using 3-MA (an inhibitor of autophagy) and with an MTT assay and Annexin V-FITC/PI staining. The results showed that inhibition of autophagy may enhance BMA-155Cl-induced apoptosis.

NF-κB, a ubiquitous transcription factor, has been implicated in the control of apoptosis and autophagy[25, 26]. NF-κB, along with many of its downstream target genes, such as the Bcl-2 family and p53, plays important roles in mediating apoptosis in response to many stimulations, including cancer therapeutic agents[24, 27, 28]. Accumulated evidence shows that the activation of NF-κB is primarily modulated by a complex formed by NF-κB and IκB in the cytoplasm of non-stimulated cells. Extracellular stimuli cause rapid phosphorylation of IκB (inhibitor of NF-κB), which is subsequently subjected to ubiquitination and proteasome degradation[29]. The complete degradation of IκB leads to rapid and transient activation of NF-κB and subsequent nuclear translocation[30]. The p53 transcription factor responds to several stimuli, such as DNA damage, hypoxia, and even oncogene activation. Activation of the p53 transcription factor can lead to the translation of various genes, which regulate cell fate by initiating cell cycle arrest, apoptosis, senescence, and even autophagy[31, 32]. The p53 protein can be modified by acetylation, phosphorylation, methylation, ubiquitination, sumoylation, neddylation, and glycosylation and is mainly degraded in the cytosol[32]. p53 can also enhance the transcription of the pro-apoptotic BH3-only proteins, Noxa and Puma, which indirectly promote Bax activation by inhibiting the function of the anti-apoptotic proteins, Bcl-2 or Bcl-xL, leading to apoptosis[30]. Emerging evidence has revealed that p53 and NF-κB signaling are linked to each other via metabolic regulation and regulation of cellular senescence and aging. WIP1 and MIF are important proteins that link p53 and NF-κB signaling cascades to each other[32]. In addition, inhibition of NF-κB abrogated p53-induced apoptosis in a p53-inducible Saos-2 cell line; the loss of p65 (a subunit of NF-κB) can also cause resistance to different agents that induce apoptosis through p53[25, 33, 34].

In this study, RT-PCR and Western blot analyses showed that BMA-155Cl increased the expression of NF-κB p65, p53, and p-p53 but decreased the expression of IκB. This finding indicates that functional NF-κB p65 and p53 are required for BMA-155Cl-mediated inhibition of the growth of HepG-2 cells. Moreover, BMA-155Cl increased NF-κB p65 levels in the nucleus but not in the cytoplasm, indicating that BMA-155Cl activated NF-κB p65, which transferred to the nucleus and positively regulated apoptosis.

To investigate the role of NF-κB p65 in BMA-155Cl-induced apoptosis and autophagy, we pretreated HepG-2 cells with BAY 11-7082. *In vitro* studies showed that the inhibition of NF-κB p65 by BAY 11-7082 decreased the expression of p53, p-p53, and the pro-apoptosis protein Bax but increased the expression of the anti-apoptosis protein Bcl-2. Our results revealed that NF-κB p65 indirectly regulated BMA-155Cl-induced apoptosis through p53 in HepG-2 cells.

Microtubule-associated protein light chain 3 (LC3), a human homolog of yeast Atg8, plays an essential role in autophagy. LC3 is cleaved to produce a cytosolic 18-kDa protein called LC3-I, which is further converted to LC3-II, a 16-kDa protein that can conjugate phosphatidylethanolamine to localize in autophagosomal membranes and is an autophagy marker[35, 36]. Enhancement of autophagy can result in the accumulation of LC3 puncta. Another important factor for autophagosome formation is Beclin-1, a 60-kDa protein encoded by the Beclin-1 gene. This protein regulates autophagosome formation through binding to class III PI3K[7]. In this study, RT-PCR and Western blot results showed that BMA-155Cl increased the expression of Beclin-1 and LC3B and the amount of LC3B that accumulated in the presence of pepstatin A, indicating the occurrence of autophagy induced by BMA-155Cl in HepG-2 cells. Moreover, inhibition of NF-κB p65 by BAY 11-7082 decreased the expression of LC3B, revealing that NF-κB p65 directly regulated BMA-155Cl-induced autophagy in HepG-2 cells.

An *in vivo* assay showed that BMA-155Cl inhibited the growth of HepG-2 tumors in mice. HE staining also verified the effective cytotoxicity of BMA-155Cl *in vivo*. Moreover, IHC results indicated increased expression of NF-κB p65, Beclin-1, LC3B, and Bax in BMA-155Cl-treated HepG-2 xenografts and decreased expression levels of Bcl-2 and IκB. This finding further confirms that BMA-155Cl can induce autophagy and apoptosis *in vivo*.

Autophagy plays an important role in protection against infections, cancers, neurodegeneration, aging, and heart diseases[7, 37, 38]. However, other studies have revealed that inhibition of autophagy is enhanced in colon cancer cells, such as human osteosarcoma U2OS cells and HeLa cells[2, 39, 40]. Thus, the role of autophagy remains controversial. The results of our study showed that inhibition of autophagy with 3-MA enhanced BMA-155Cl-induced apoptosis in HepG-2 cells, thereby suggesting that BMA-155Cl induced a temporary protective autophagy followed by apoptosis. The experimental conditions in this study were strictly controlled to minimize the influence of the environment or external stimuli on cell autophagy[41].

In conclusion, this study is the first to report that BMA-155Cl produced growth inhibition in several types of cancer cells and induced a temporary protective autophagy, followed by apoptosis associated with the NF-κB p65 signaling pathway, in HepG-2 cells both *in vitro* and *in vivo*. We speculate that NF-κB p65 regulated the expression of the autophagy-associated protein LC3B and controlled the expression of p53 to control the expression of Bcl-2 family proteins in BMA-155Cl-induced HepG-2 cells. Considering the complexity of intracellular signal transduction, other signaling proteins,

such as p38 and AKT, may also play important roles in BMA-155Cl-induced autophagy and apoptosis in HepG-2 cells[42]. Our results suggest that the BMA-155Cl-induced inhibition of HepG-2 cell growth via autophagy and apoptosis might be a promising anti-tumor candidate. Hence, BMA-155Cl could be a promising pro-apoptotic compound for developing novel anticancer drugs.

Acknowledgements

Author contribution

Prof Xia LI designed the research and revised the manuscript. Xiao SUN and Lin LI conducted the research, analyzed the data and wrote the paper. Hong-guang MA and Wei-ming ZHU provided the compounds. Pu SUN, Qi-lin WANG, and Ting-ting ZHANG assisted with portions of the research. Yue-mao SHEN supported the revised work.

References

1   Ouyang L, Shi Z, Zhao S, Wang FT, Zhou TT, Liu B, *et al*. Programmed cell death pathways in cancer: a review of apoptosis, autophagy and programmed necrosis. Cell Prolif 2012; 45: 487–98.

2   Li X, Wu WKK, Sun B, Cui M, Liu S, Gao J, *et al*. Dihydroptychantol a, a macrocyclic bisbibenzyl derivative, induces autophagy and following apoptosis associated with p53 pathway in human osteosarcoma U2OS cells. Toxicol Appl Pharmacol 2011; 251: 146–54.

3   Fuchs Y, Steller H. Live to die another way: modes of programmed cell death and the signals emanating from dying cells. Nat Rev Mol Cell Biol 2015; 16: 329–44.

4   Shin SY, Hyun J, Yu JR, Lim Y, Lee YH. 5-methoxyflavanone induces cell cycle arrest at the G_2/M phase, apoptosis and autophagy in HCT116 human colon cancer cells. Toxicol Appl Pharmacol 2011; 254: 288–98.

5   Paglin S, Hollister T, Delohery T, Hackett N, Mcmahill M, Sphicas E, *et al*. A novel response of cancer cells to radiation involves autophagy and formation of acidic vesicles. Cancer Res 2001; 61: 439–44.

6   Mathias T. The role of autophagy in tumour development and cancer therapy. Expert Rev Mol Med 2009; 11: e36.

7   Wang K. Autophagy and apoptosis in liver injury. Cell Cycle 2015; 14: 1631–42.

8   Wei M, Li Z, Yang Z. Crosstalk between protective autophagy and NF-κB signal in high glucose-induced podocytes. Mol Cell Biochem 2014; 394: 261–73.

9   Yin QH, Yan FX, Zu XY, Wu YH, Wu XP, Liao MC, *et al*. Anti-proliferative and pro-apoptotic effect of carvacrol on human hepatocellular carcinoma cell line HepG-2. Cytotechnol 2012; 64: 43–51.

10   Xu Y, Qin X, Zhou J, Tu Z, Bi X, Li W, *et al*. Tissue factor pathway inhibitor-2 inhibits the growth and invasion of hepatocellular carcinoma cells and is inactivated in human hepatocellular carcinoma. Oncol Lett 2011; 2: 779–83.

11   Pierce LT, Cahill MM, Winfield HJ, Mccarthy FO. Cheminform abstract: synthesis and identification of novel indolo[2,3-a]pyrimido[5,4-c] carbazoles as a new class of anticancer agents. Eur J Med Chem 2012; 56: 292–300.

12   Wang K, Chen LXG, Liu ZZ. Synthesis and antitumor activity of bis-indolylmaleimide and amino acid ester conjugates. J Asian Nat Prod Res 2010; 12: 36–42.

13   Wang K, Liu ZZ. Synthesis and cytotoxic activities of a series of novel n-methyl-bisindolylmaleimide amide derivatives. J Asian Nat Prod Res 2014; 16: 296–303.

14   Wang K, Liu Z. Cheminform abstract: synthesis of arcyriarubin A (vi) and arcyriaflavin A (vii) via cross-coupling of indolylboronic acid with dibromomaleimides. Synth Commun 2009; 40: 144–50.

15   Sun Y, Zou M, Chen H, Qin Y, Song X, Lu N, *et al*. Wogonoside induces autophagy in MDA-MB-231 cells by regulating MAPK-mTOR pathway. FASEB J 2012; 51: 53–60.

16   Liu MC, Lin TH, Wu TS, Yu FY, Lu CC, Liu BH. Aristolochic acid I suppressed inos gene expression and NF-κB activation in stimulated macrophage cells. Toxicol Lett 2011; 202: 93–9.

17   Wang QS, Xiang Y, Cui YL, Lin KM, Zhang XF. Dietary blue pigments derived from genipin, attenuate inflammation by inhibiting LPS-induced iNOs and COX-2 expression via the NF-κB inactivation. PLoS One 2012; 7: e34122.

18   Zhang T, Bo J, Zou ST, Liu F, Dong H. Overexpression of B7-H3 augments anti-apoptosis of colorectal cancer cells by JAK2-stat3. Word J Gastroenterol 2015; 21: 1804–13.

19   Liang XH, Jackson S, Seaman M, Brown K, Kempkes B, Hibshoosh H, *et al*. Induction of autophagy and inhibition of tumorigenesis by Beclin 1. Nature 2000; 402: 672–6.

20   Soumaoro LT, Iida S, Uetake H, Ishiguro M, Takagi Y, Higuchi T, *et al*. Expression of 5-lipoxygenase in human colorectal cancer. World J Gastroenterol 2006; 12: 6355–60.

21   Chandel NS, Trzyna WC, Mcclintock DS, Schumacker PT. Role of oxidants in NF-kappa B activation and TNF-alpha gene transcription induced by hypoxia and endotoxin. J Immunol 2000; 165: 1013–21.

22   Wu C, Wang P, Rao J, Wang Z, Zhang C. Triptolide alleviates hepatic ischemia/reperfusion injury by attenuating oxidative stress and inhibiting NF-κB activity in mice. J Surg Res 2010; 166: 205–13.

23   Roy S, Roy S, Gribble GW. A practical method for the synthesis of indolylaryl- and bisindolylmaleimides (v). Org Lett 2007; 38: 4975–7.

24   Bonvin C, Guillon A, van Bemmelen MX, Gerwins P, Johnson GL, Widmann C. Role of the amino-terminal domains of mekks in the activation of NF kappa B and MAPK pathways and in the regulation of cell proliferation and apoptosis. Cell Signal 2002; 14: 123–31.

25   Zhang Y, Wu Y, Di W, Tashiro SI, Onodera S, Ikejima T. NF-κB facilitates oridonin-induced apoptosis and autophagy in HT1080 cells through a p53-mediated pathway. Arch Biochem Biophys 2009; 489: 25–33.

26   Liao G, Gao B, Gao Y, Yang X, Cheng X, Ou Y. Phycocyanin inhibits tumorigenic potential of pancreatic cancer cells: role of apoptosis and autophagy. Sci Rep 2016; 6: 34564.

27   Fujioka S, Schmidt C, Sclabas GM, Li Z, Pelicano H, Peng B, *et al*. Stabilization of p53 is a novel mechanism for proapoptotic function of NF-kappaB. J Biol Chem 2004; 279: 27549–59.

28   Liu YH, Liu GH, Mei JJ, Wang J. The preventive effects of hyperoside on lung cancer *in vitro* by inducing apoptosis and inhibiting proliferation through caspase-3 and p53 signaling pathway. Biomed Pharmacother 2016; 83: 381–91.

29   Pei YY, Chuang SE, Yeh KH, Ying CS, Ea CK, Cheng AL. Increase of the resistance of human cervical carcinoma cells to cisplatin by inhibition of the MEK to ERK signaling pathway partly via enhancement of anti-cancer drug-induced NFκB activation. Biochem Pharmacol 2002; 63: 1423–30.

30   Liu S, Wu D, Li L, Sun X, Xie W, Li X. Nf-κb activation was involved in reactive oxygen species-mediated apoptosis and autophagy in 1-oxoeudesm-11(13)-eno-12,8α-lactone-treated human lung cancer cells. Arch Pharm Res 2014; 37: 1039–52.

31 Ak P, Levine AJ. P53 and NF-κB: Different strategies for responding to stress lead to a functional antagonism. FASEB J 2010; 24: 3643–52.

32 Salminen A, Kai K. Control of p53 and NF-κB signaling by wip1 and mif: role in cellular senescence and organismal aging. Cell Signal 2011; 23: 747–52.

33 Ryan KM, Ernst MK, Rice NR, Vousden KH. Role of NF-kappaB in p53-mediated programmed cell death. Nature 2000; 404: 892–7.

34 Ryan KM, O'Prey J, Vousden KH. Loss of nuclear factor-kappab is tumor promoting but does not substitute for loss of p53. Cancer Res 2004; 64: 4415–8.

35 Levine B, Mizushima N, Virgin HW. Autophagy in immunity and inflammation. Nature 2011; 469: 323–35.

36 Sanjuan MA, Dillon CP, Tait SWG, Simon M, Frank D, Samuel C, *et al*. Toll-like receptor signalling in macrophages links the autophagy pathway to phagocytosis. Nature 2007; 450: 1253–7.

37 Tsuchihara K, Fujii S, Esumi H. Autophagy and cancer: dynamism of the metabolism of tumor cells and tissues. Cancer Lett 2009; 278: 130–8.

38 Kundu M, Thompson CB. Autophagy: basic principles and relevance to disease. Annu Rev Pathol 2008; 3: 427–55.

39 Bauvy C, Gane P, Arico S, Codogno P, Ogier-Denis E. Autophagy delays sulindac sulfide-induced apoptosis in the human intestinal colon cancer cell line HT-29. Exp Cell Res 2001; 268: 139–49.

40 Cui Q, Tashiro S, Onodera S, Ikejima T. Augmentation of oridonin-induced apoptosis observed with reduced autophagy. J Pharmacol 2006; 101: 230–9.

41 Lin CJ, Lee CC, Shih YL, Lin TY, Wang SH, Lin YF, *et al*. Resveratrol enhances the therapeutic effect of temozolomide against malignant glioma *in vitro* and *in vivo* by inhibiting autophagy. Free Radic Biol Med 2012; 52: 377–91.

42 Lin Z, Liu T, Kamp DW, Wang Y, He H, Zhou X, *et al*. Akt/mTOR and c-jun N-terminal kinase (JNK) signaling pathways are required for chrysotile asbestos-induced autophagy. Free Radic Biol Med 2014; 72: 296–307.